Journal of Hydroscience and Hydraulic Engineering
Vol. 8, No. 2, December, 1990, 1-20

OPEN CHANNEL FLOW WITH SPATIALLY VARIED BED SHEAR STRESS

By

Tetsuro TSUJIMOTO

Associate Professor, Department of Civil Engineering, Kanazawa University
2-40-20, Kodatsuno, Kanazawa, 920, Japan

António H. CARDOSO

Laboratório Nacional de Engenharia Civil
Avenida do Brasil, 101, 1799, Lisboa Codex, Portugul

and

Akira SAITO

Shimizu Construction Corporation, Ltd.
Tokyo, 108, Japan

ABSTRACT

Bed forms and sorting of the fluvial beds induce the spatial change in the bed shear stress, and subsequently the turbulent characteristics and the sediment transport respond it with spatial lag. The effects of the spatial acceleration or deceleration should be classified into the direct one due to the spatial derivative of the bed shear stress and the indirect one due to the so-called response lag: The latter is mainly investigated in this paper. A relaxation model with a concept of the impulse response is prepared for the transition process of the Reynolds-stress distribution, and the degeneration of the turbulent characteristics of the spatially accelerated or decelerated flow is discussed based on it. Moreover, the flume experiments of the flow with spatial acceleration and/or deceleration are carried out, and the results are discussed mainly based on the present relaxation model.

INTRODUCTION

The flow over bed forms repeats spatial acceleration and deceleration, and thus, the turbulent characteristics and the subsequent behavior of sediment become quite different from those in uniform flow. As an example for the flow over dunes, several works were done by focussing the development of the so-called internal boundary layer on the individual dunes (Ishikawa (7), Tsujimoto & Nakagawa (21), McLean & Smith (10), Nakagawa et al. (12)). Certainly, when one is interested in bed-load motion, such an approach is available. However, the length scale for the bed shear stress to reach equilibrium is much shorter than that for the velocity distribution or the turbulence characteristics of the flow in the region far from the bed. When one takes the example of flow with an abrupt change of bed roughness, which was previously studied by Antonia (1,2) , Townsend (18) and others, the change of the bed shear stress is rather immediate (Jacobs (8), Kanda et al. (9), Nezu et al. (15)) while the Reynolds stress distribution adapts to it gradually and its adaptation or relaxation length increases with the distance from the bed. Particularly, at the height near the water surface in the case of open channel flow, it reaches more than 100 times flow depth for 90% relaxation.

The effect of the spatial acceleration can be divided into the following two: (i) the direct effect; the spatial derivative of the bed shear stress degenerates the velocity profile; and (ii) the indirect effect due to relaxation. The effect (i) is determined locally; while the effect (ii) becomes a function of the longitudinal distance.

When the velocity distribution has no relaxation property or is determined only by the local parameters, it is in general expressed as follows:

$$\frac{u}{u_*} = \phi_1\left(\frac{u_* y}{\nu}\right) + \phi_2\left(\frac{y}{h}\right) \tag{1}$$

in which u=local velocity; u_*=shear velocity; y=distance from the bed; ν=kinematic viscosity; and h=flow depth. In general, ϕ_1 is termed the "wall law" and the log low is applied; while ϕ_2 corresponds to the so-called wake law.

The log law is written as

$$\phi_1\left(\frac{u_* y}{\nu}\right) = A \ln \frac{u_* y}{\nu} + B \tag{2}$$

in which A is a universal constant (A=1/κ; κ=Kármán constant) and B is also a constant determined by the bed conditions. While, the so-called Coles' wake law (5) is written as

$$\phi_2\left(\frac{y}{h}\right) = \frac{2\Pi}{\kappa} \sin^2\left(\frac{\pi y}{2h}\right) \tag{3}$$

in which Π is called the wake-strength parameter. Eq.3 is an increasing function of y/h. The direct effect will appear as the changes of some of the parameters involved in Eqs.2 and 3, or A, B and Π. Referring the previous experiments including pipe flows, A and B would be hardly affected by the spatial derivative of bed shear stress, in other words, by the pressure gradient; while Π might be significantly affected apparently.

Even if the indirect effect appears, the wall law would not be degenerated, because the slow relaxation becomes dominant far from the bed. Hence, apparently Π must be affected by relaxation, though, exactly saying, the functional form of the right part of Eq.3 becomes different from the original one. And, what should be emphasized is that Π becomes a function of the longitudinal distance.

In this study, the spatial lag in response of the Reynolds-stress distribution to the change of the bed shear stress is firstly focussed. The Reynolds-stress distribution just downstream of an abrupt change of bed roughness is no longer triangular (as seen by Jacobs' experiments (see Fig.1, (7)) often included in text books, such as "Boundary-Layer Theory" by Schlichting). The velocity profile is intimately related to the Reynolds-stress distribution, and thus the velocity distribution of flow over spatially varied bed shear stress cannot be represented by the well-known log law. In this paper, a reasonable model to describe the transition process of the Reynolds stress distribution is proposed and tested.

The responses of the Reynolds stress and the velocity distributions to an abrupt change of bed roughness in open channels were investigated theoretically (Antonia & Luxton (1,2), Townsend (17) and others) and by turbulence measurements (Kanda et al. (9), Nezu et. al. (15)), and interesting results were obtained up to date. These data will be used to verify the model proposed in this paper.

Moreover, the flow with spatial acceleration or/and deceleration is investigated experimentally. Based on the experimental data, the applicability and the limitation of the "relaxation model" are inspected.

RELAXATION MODEL

As seen from the experiments of Jacobs (8) (see Fig.1; The dashed curves in the figure are the calculated results by using Jacobs' empirical formula), the response of the Reynolds stress to the change in the bed roughness is faster in the region near the bed and slower in the region far from the bed. In other words, the relaxation scale of the Reynolds stress increases with the distance from the bed. The impulse response is defined for each value of the relative height (η≡y/h; y= distance from the bed where the Reynolds stress becomes 0 and that implies the flow depth in the case of open channel flow). The relaxation model is written as follows:

$$\tau(\eta\,|\xi) = \int_0^\infty \tau_e(\eta\,|\xi-\delta) \cdot g_R(\delta\,|\eta)\, d\delta \tag{4}$$

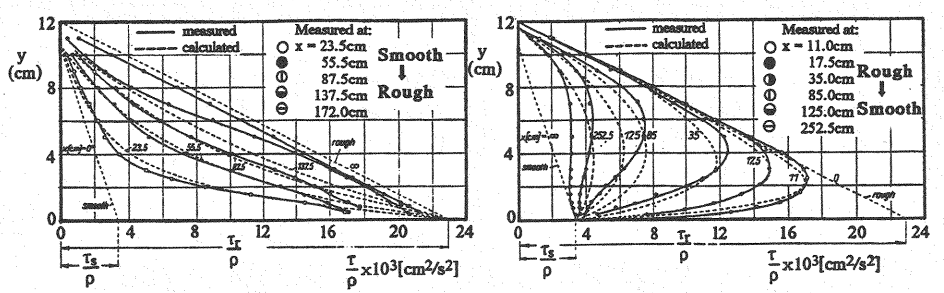

Fig.1 Transition process of Reynolds-stress distribution by Jacobs' wind-tunnel experiments

in which $\tau(\eta|\xi)$=Reynolds-stress distribution at ξ; $\xi \equiv x/h$; x=longitudinal distance; $\tau_e(\eta|\xi)$= equilibrium Reynolds-stress distribution; and $g_R(\delta|\eta)$=impulse response of Reynolds stress at the relative height η. The impulse response is often approximated by an exponential function as follows:

$$g_R(\xi|\eta) = \frac{1}{\Lambda(\eta)} \exp\left[-\frac{\xi}{\Lambda(\eta)}\right] \tag{5}$$

in which $\Lambda(\eta)$=relaxation scale non-dimensionalized by h at the relative height η.

Under equilibrium, the Reynolds-stress distribution is triangular, and thus Eq.4 is rewritten as

$$\tau(\eta|\xi) = (1-\eta)\int_0^\infty \tau_b(\xi-\delta)\cdot g_R(\delta|\eta)d\delta \equiv (1-\eta)\cdot\tau_b(\xi)\cdot\Omega(\eta|\xi) \tag{6}$$

$$\Omega(\eta|\xi) \equiv \frac{\int_0^\infty \tau_b(\xi-\delta)\cdot g_R(\delta|\eta)d\delta}{\tau_b(\xi)} = \int_0^\infty \psi_b(\xi-\delta)\cdot g_R(\delta|\eta)d\delta \tag{7}$$

in which $\tau_b(\xi)$=longitudinal change of bed shear stress; and $\psi_b(\xi-\delta)\equiv\tau_b(\xi-\delta)/\tau_b(\xi)$. $\Omega(\eta)$ represents the deviation of the Reynolds-stress profile from the equilibrium profile $(1-\eta)\tau_b$.

An abrupt change of bed roughness can be regarded as a rectangular change of $\tau_b(\xi)$ though somewhat over-shooting phenomenon appears just downstream of the abrupt change of the bed roughness (Nezu et al. (15)). When the bed shear stress changes abruptly from τ_{b1} to τ_{b2} at ξ=0, Eq.6 describes the transition process of the Reynolds-stress distribution as follows:

$$\tau(\eta|\xi) = (1-\eta)\left[\tau_{b1}\int_\xi^\infty g_R(\delta|\eta)d\delta + \tau_{b2}\int_0^\xi g_R(\delta|\eta)d\delta\right] \tag{8}$$

If Eq.5 is applied for $g_R(\xi|\eta)$,

$$\tau(\eta|\xi) = (1-\eta)\left\{\tau_{b1}\exp\left(-\frac{\xi}{\Lambda(\eta)}\right) + \tau_{b2}\left[1-\exp\left(-\frac{\xi}{\Lambda(\eta)}\right)\right]\right\} \tag{9}$$

or

$$\frac{\tau(\eta|\xi)-\tau_{b1}(1-\eta)}{(\tau_{b2}-\tau_{b1})(1-\eta)} = 1-\exp\left[-\frac{\xi}{\Lambda(\eta)}\right] \tag{10}$$

For each relative height, the adaptation of Eq.10 to the data of Jacobs, which was obtained in the wind-tunnel experiments, has been inspected and the following equation as for $\Lambda(\eta)$ has been proposed (see Fig.2):

$$\Lambda(\eta) = 20\eta(1+1.5\eta^3) \qquad (11)$$

As shown in Fig.3, the experimental data on the transition of the Reynolds-stress distribution can be well described by Eq.9 with Eq.11.

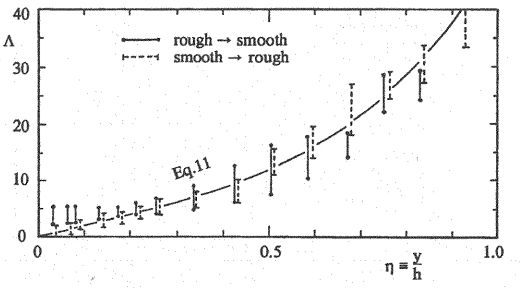

Fig.2 Variation of relaxation scale with the relative height

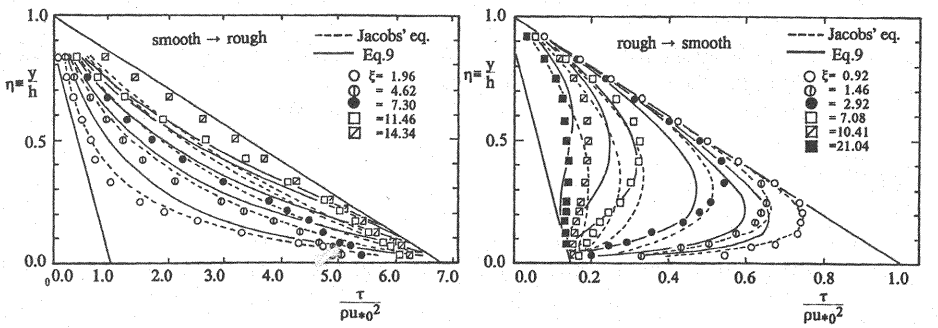

Fig.3 Applicability of the relaxation model to Jacobs' data

VELOCITY DISTRIBUTION AND TURBULENCE INTENSITY

When the non-equilibrium profile of the Reynolds stress is known, the velocity profile might be obtained by applying the following mixing length model:

$$\frac{\partial u^+(\xi,\eta)}{\partial \eta} = \frac{1}{\ell^*}\sqrt{\frac{\tau(\xi,\eta)}{\rho u_{*r}^2}} \qquad (12)$$

in which $u^+ \equiv u/u_{*r}$; u_{*r}=shear velocity at the representative section; u=local velocity; $\ell^* \equiv \ell/h$; and ℓ=mixing length. For an open channel flow, the mixing length is appropriately and phenomenologically assumed as $\ell^* = \kappa\eta\sqrt{1-\eta}$. With the above-explained mixing length model and the non-equilibrium Reynolds-stress distribution as expressed by Eq.6, we deduce a velocity profile by integrating the following equation.

$$\frac{\partial u^+(\xi,\eta)}{\partial \eta} = \frac{1}{\kappa\eta}\sqrt{\Omega(\eta,\xi)} \qquad (13)$$

in which the representative section is defined locally. That means that u^+ is the velocity non-dimensionalized by the local shear velocity ($\sqrt{\tau_b(\xi)/\rho}$). Eq.13 implies that the velocity profile will be different from the log law unless Ω is constant along η. Even if Ω is constant along η, an apparent Kármán constant ($\kappa' = \kappa/\Omega$) is no longer universal unless Ω=1.

If the correlation coefficient of the longitudinal and the vertical components of velocity fluctuation, $r_T(\eta)$, is known, the Reynolds-stress and the turbulence intensity are related to each other as follows:

$$\tau = -\rho r_T(\eta) \cdot u'_{rms} \cdot v'_{rms} \qquad (14)$$

in which u'_{rms}, v'_{rms}=longitudinal and vertical components of turbulence intensity. The ratio of u'_{rms} to v'_{rms} is to be represented by $K_{uv}(\eta)$. When the non-equilibrium profile of the Reynolds stress is

expressed as Eq.6, the profiles of the turbulence intensities are expressed as follows if $K_{uv}(\eta)$ and $r_T(\eta)$ are known:

$$\frac{u'_{rms}(\eta|\xi)}{u_*}=\sqrt{\frac{K_{uv}(\eta)}{r_{T*}(\eta)}}\cdot\sqrt{\Omega(\eta|\xi)}\ ;\qquad \frac{v'_{rms}(\eta|\xi)}{u_*}=\sqrt{\frac{1}{K_{uv}(\eta)\cdot r_{T*}(\eta)}}\cdot\sqrt{\Omega(\eta|\xi)} \tag{15}$$

in which $r_{T*}(\eta)\equiv r_T(\eta)/(1-\eta)$; and u_* is defined locally ($u_*=\sqrt{\tau_b(\xi)/\rho}$).

In the case of uniform turbulent flow, the Reynolds-stress distribution is equilibrium and thus expressed as $\rho u_*^2(1-\eta)$, while, according to Townsend's model of turbulence (17), the turbulence intensity is expressed as

$$\frac{u'_{rms}}{u_*}=2.3\exp(-\eta)\ ;\qquad \frac{v'_{rms}}{u_*}=1.27\exp(-\eta) \tag{16}$$

in which the numerical values of the parameters empirically proposed by Nezu (14) are adopted. Then, the correlation coefficient, r_T, is expressed as

$$r_T(\eta)=-0.342(1-\eta)\exp(2\eta)\equiv r_{T*}(\eta)\cdot(1-\eta) \tag{17}$$

According to Nakagawa et al. (13), Eq.16 is not necessarily valid in the near-bed region called "roughness sublayer" for flow with small relative submergence, but Eq.17 is still valid in the roughness sublayer. This fact suggests that Eq.17 may be also applied to non-equilibrium as far as it is less severe. Furthermore, Nakagawa et al. (13) inspected the relation between u'_{rms} and v'_{rms} in the roughness sublayer, where Eq.15 is no longer valid, but found that the ratio of u'_{rms} to v'_{rms}, K_{uv}, is still kept almost constant (K_{uv}=2.3/1.27). Thus, it is assumed here that

$$K_{uv}(\eta)=\frac{2.3}{1.27} \tag{18}$$

Substituting Eqs.17 and 18 into Eq.15, we obtain the following profile of the turbulence intensities under non-equilibrium conditions.

$$\frac{u'_{rms}}{u_*}=2.3\sqrt{\Omega(\eta|\xi)}\cdot\exp(-\eta)\ ;\qquad \frac{v'_{rms}}{u_*}=1.27\sqrt{\Omega(\eta|\xi)}\cdot\exp(-\eta) \tag{19}$$

COMPARISON WITH DATA OF OPEN CHANNEL FLOW WITH ABRUPT CHANGE OF BED ROUGHNESS

Recently, an accurate data set of turbulence measurements in open channel accomplished with a laser Doppler anemometer (LDA) was obtained by Nezu et al. (15). The applicability of the Reynolds-stress relaxation model proposed in the present study of which parameter has been determined for wind-tunnel data (Jacobs' data (8)) to open channel flow is inspected here.

The experiments were conducted in a 10m long and 0.40m wide straight flume equipped at Kyoto University, and the bottom roughness was changed at the middle of the flume length. The rough part was made of closely packed glass beads of 1.2cm diameter; while the smooth part was a steel plate. The surface of the steel plate was adjusted to the level 0.2d (d=diameter of glass beads) below the top of the roughness (theoretical wall), and uniform flow along the total length of the flume could be established approximately by adjusting a weir at the downstream end of the flume. The experimental conditions are summarized as follows: i_b=0.00015~0.00207; h≅6.0cm; U=15.33~30.67cm/s; u_*=0.71~ 2.39cm/s; and $\beta\equiv u_{*2}/u_{*1}\cong 0.55$ for "rough to smooth" condition, while $\beta\cong 1.8$ for "smooth to rough" condition, in which i_b=bed slope; U=cross-sectionally averaged velocity; h=flow depth; and u_{*1}, u_{*2}=shear velocities of the equilibrium flows before and after the change of roughness, respectively. The value of u_* is determined from an extrapolation of the measured Reynolds stress to the bed.

In the flow with an abrupt change of bed roughness, the bottom shear stress changes almost immediately to respond to the change of the roughness, though somewhat over-shooting phenomenon has been reported (Nezu et al. (15)). The over-shooting is actually important to investigate the problems

such as local scour at the joint of the beds with different roughness, but the effect may be spatially limited, and as far as the present discussion is concerned the immediate response of the bed shear stress to the change of the bed roughness is reasonably assumed.

When the shear velocity changes from u_{*1} to u_{*2} ($u_{*2}\equiv\beta u_{*1}$) abruptly at $\xi=0$, the transition process of the Reynolds-stress distribution is written as follows based on Eq.8:

$$\frac{\tau(\eta\,|\xi)}{\rho u_{*1}^2} = (1-\eta)[(\beta^2-1)\cdot\Psi(\eta\,|\xi)+1] \equiv (1-\eta)\cdot\Theta(\eta\,|\xi) \tag{20}$$

in which

$$\Psi(\eta\,|\xi) = \int_0^{\xi} g_R(\delta\,|\eta)d\delta = 1 - \exp\left[-\frac{\xi}{\Lambda(\eta)}\right] \tag{21}$$

and an exponential type impulse response (Eq.5) has been assumed. $\Theta(\eta\,|\xi)$ in this case corresponds to $(u_{*2}/u_{*1})^2\Omega(\eta\,|\xi)=\beta^2\Omega(\eta\,|\xi)$. $\Theta(\eta\,|\infty)\rightarrow\beta^2$. Thus, when $\xi<0$ or $\xi\rightarrow\infty$, the equilibrium appears.

Figure 4 shows a comparison between the measured data and the calculated curves of the Reynolds-stress distribution, and a good agreement between them is recognized. That means that the impulse response determined based on the data obtained in the wind tunnel can be applied to open channel flow without any modifications.

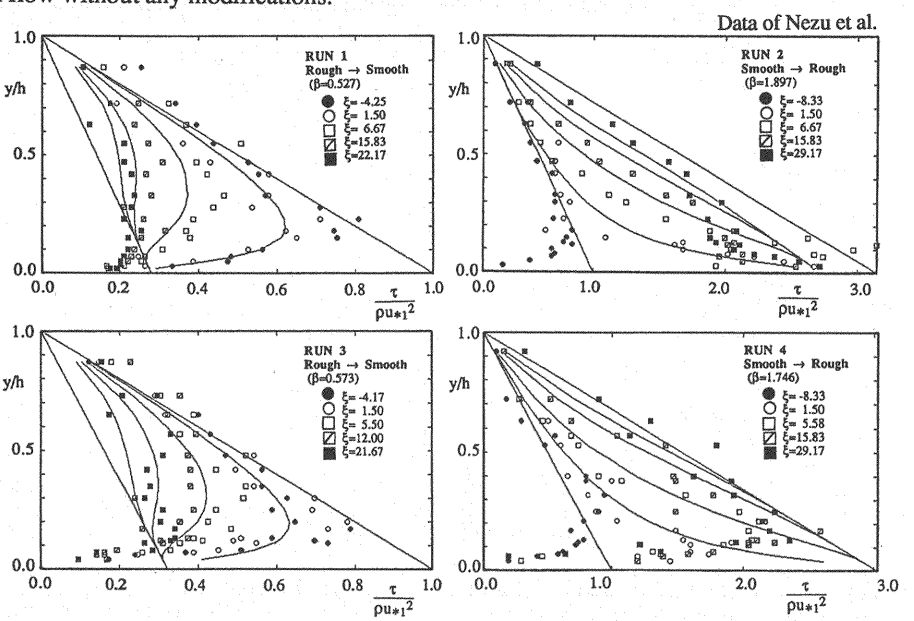

Fig.4 Transition of Reynolds-stress distribution due to abrupt change of bed roughness

The velocity distribution is obtained based on the present model. Eq.12 is rewritten as follows for this case:

$$\frac{\partial}{\partial\eta}\left[\frac{u(\eta\,|\zeta)}{u_{*1}}\right] = \frac{1}{\kappa\eta}\sqrt{\Theta(\eta\,|\xi)} \tag{22}$$

The velocity profile was calculated with Eq.22, where the boundary condition was determined so that U/u_* remained constant in this case because the depth of the flow hardly changed in the transition process. The calculated velocity distribution is compared with the measured distribution in Fig.5, and it shows a good agreement between them. The velocity distribution adapts to the log-law corresponding to

the new bed roughness from the log-law corresponding to the bed roughness of the upstream reach increasingly. The response in the region near the bed is fast and it delays more and more with the distance from the bed.

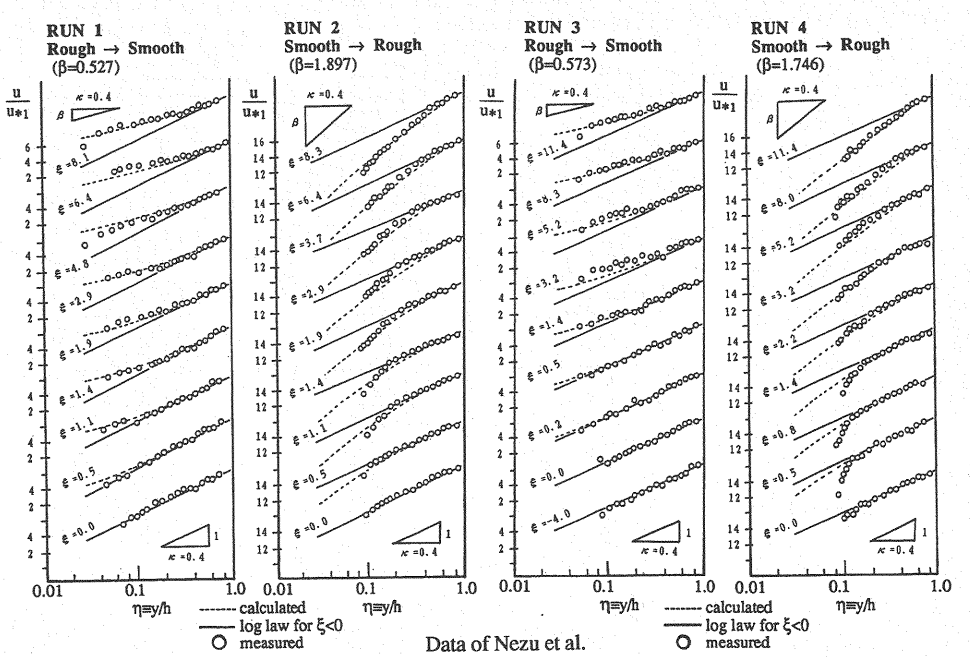

Fig.5 Longitudinal change of velocity profile due to abrupt change of bed roughness

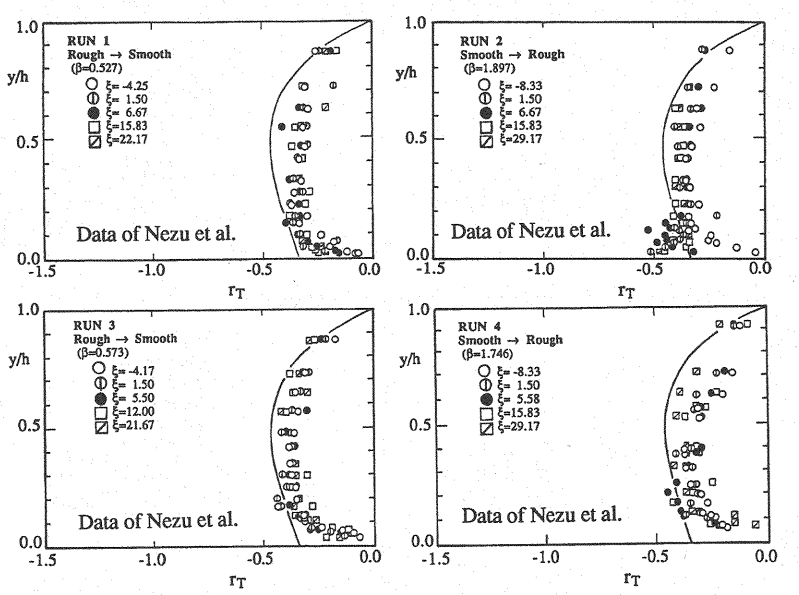

Fig.6 Distribution of the correlation coefficient of turbulence in x and y directions along the flow depth

Figure 6 shows the correlation coefficient between the turbulence intensity in the longitudinal direction and that in the vertical direction, and it can be regarded as almost universal even in the transition process of the Reynolds stress distribution. Moreover, the ratio of the turbulence intensity in the longitudinal direction to that in the vertical direction is almost constant along the flow depth even in the transition process as similarly as under equilibrium, as shown in Fig.7. These results suggest that the profiles of the turbulence intensities are written as

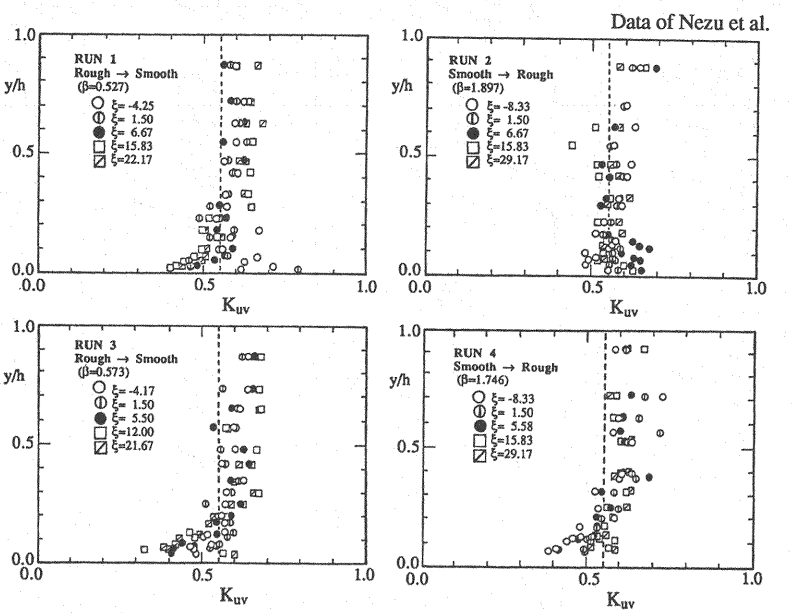

Fig.7 Distribution of the ratio of turbulence intensity in x direction to that in y direction along the flow depth

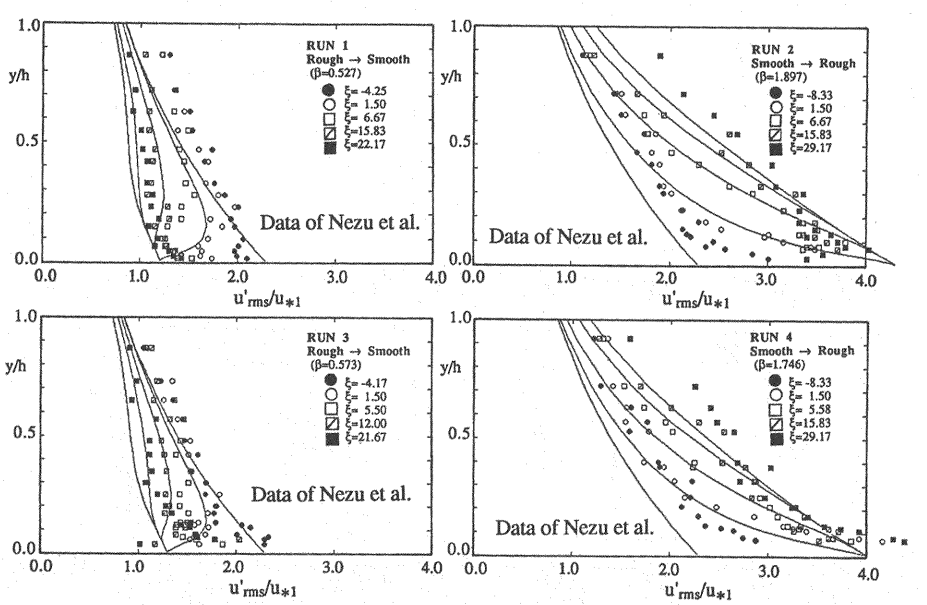

Fig.8(a) Distribution of turbulence intensity in x direction along the flow depth

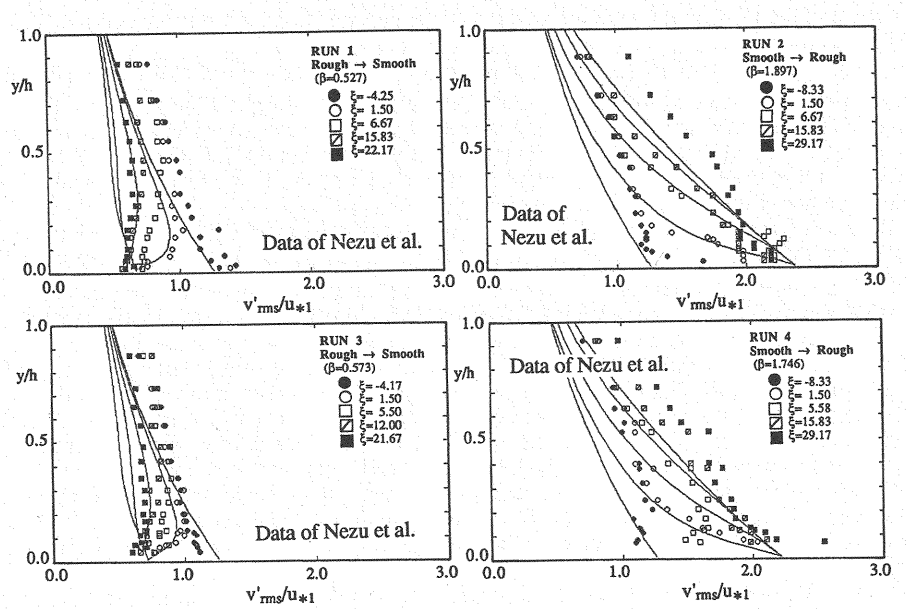

Fig.8(b) Distribution of turbulence intensity in y direction along the flow depth

$$\frac{u'_{rms}}{u_{*1}} = 2.3\sqrt{\Theta(\eta|\xi)}\cdot\exp(-\eta)\ ;\quad \frac{v'_{rms}}{u_{*1}} = 1.27\sqrt{\Theta(\eta|\xi)}\cdot\exp(-\eta) \qquad (23)$$

and these are well consistent with the experimental data as shown in Fig.8.

EXPERIMENTS OF FLOW WITH SPATIAL ACCELERATION AND DECELERATION

The experiments were carried out in a 12m long, 0.4m wide tilting flume at Kanazawa University. In the flume, the accelerating and/or the decelerating units were arranged as illustrated in Fig.9. These units and the bed of the other reaches of the flume were made out of acrylic plates. The test reach is divided into three parts: (A) the upstream region with the slope of the flume; (B) the region with different slope (adverse or favorable) where the flow is decelerated or accelerated; and (C) the downstream region with the same slope to the flume. The flows in the regions (A) and (C) are quasi-uniform while the flow in the region (B) is accelerated or decelerated. The length of the region (B), L, and the difference in the height between the regions (A) and (C), H, are indicated in Fig.9. The coordinate x is measured longitudinally from the upstream end of the region (B), and x_c denotes the downstream end of the region (B).

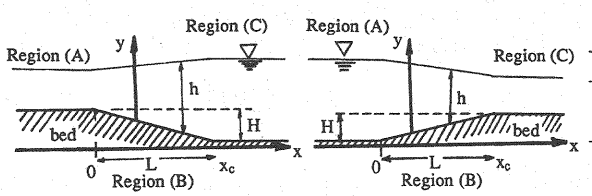

CASE	L (cm)	H (cm)
A	91.3	4.90
B	91.3	4.90
C	91.3	1.00

Fig.9 Spatial accelerating and decelerating flow parts in the flume

In the experiments, the velocity was measured by a propeller currentmeter of 3mm diameter (SV-3, Shinozuka). The output from the currentmeter was recorded by a digital recorder (DRF-1, TEAC) during about 45s at 50Hz. Even in the region (B) the bed slope was small, and thus, only the velocity parallel to the x axis was measured, and y was measured perpendicularly to the x axis. At several sections, the distributions of the time-averaged velocity and the longitudinal component of the turbulence

intensity, and the flow depth were measured. The experimental conditions are summarized as follows: i_b=0.0005~0.001; h=4.2~11.3cm; and U=12.5~45.5cm/s.

The local shear velocity (u_*) was estimated by applying the log law to the data near the bed based on reasoning that the effect of acceleration in the wall region might be negligible. The longitudinal change of the estimated shear velocity is shown in Fig.10. In the regions (A) and (C), the shear velocity is almost constant; while in the region (B) it obviously varies, but the spatial derivative of the bed shear stress is roughly constant. Flow acceleration accompanies the increase of the shear velocity while deceleration does the decrease of the shear velocity.

Figure 11 shows some examples of the measured velocity profile in the dimensionless versions by using u_* estimated by the aforementioned method. According to Fig.11, the velocity profile follows well the log law (Eq.2) where A=2.5 (1/κ) and B=5.5 (Nikuradse's value for hydraulically smooth flow regime) in the region (A). In the region (B), the velocity profile normalized by the local shear velocity becomes different from the log law and it changes with the longitudinal distance though the changes of the spatial derivative of the shear velocity is not so evident. That suggests the relaxation effect in this region. In the case of acceleration, the velocity profile becomes more uniform than the log-law increasingly in the region far from the bed. The velocity profile in semi-log coordinates looks to change as a clockwise rotation. On the other hand, in the case of deceleration, the velocity gradient in the region far from the bed increases with the longitudinal distance, and the change of the profile in semi-log coordinates looks an anti-clockwise rotation. In both cases, the velocity near the bed normalized by the local shear velocity remains constant against x. In the region (C), the velocity profile degenerated by the relaxation effect tends to return back to the log law gradually. The reverse process is faster in the lower layer, but the reverse process in general is extremely slow. Even after the distance twice the length of the region (B), the reverse process is accomplished a half at most. In the region (C), the spatial derivative of the bed shear stress is almost zero, nevertheless the velocity profile is still apart from the log law. That suggests the strong effect of relaxation.

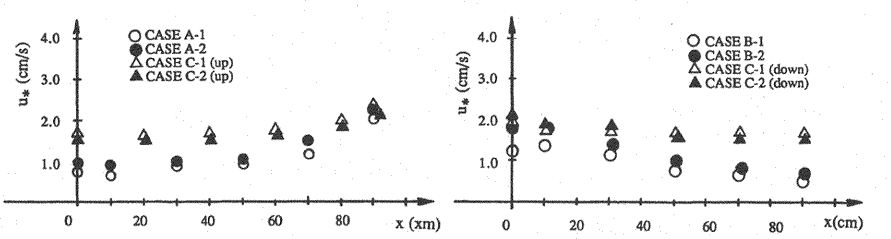

Fig.10 Longitudinal variation of shear velocity in Region (B)

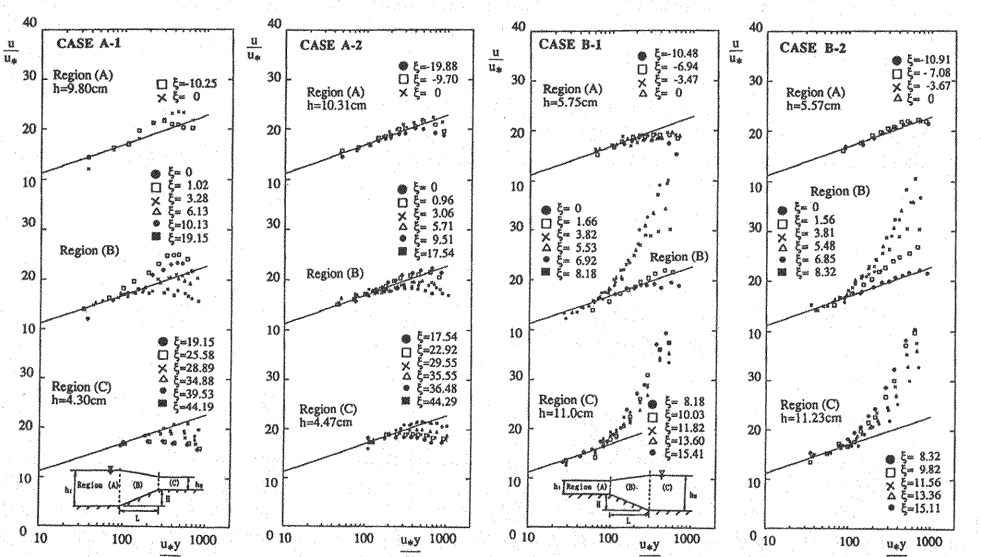

Fig.11 Longitudinal change of velocity profile by spatial acceleration or deceleration

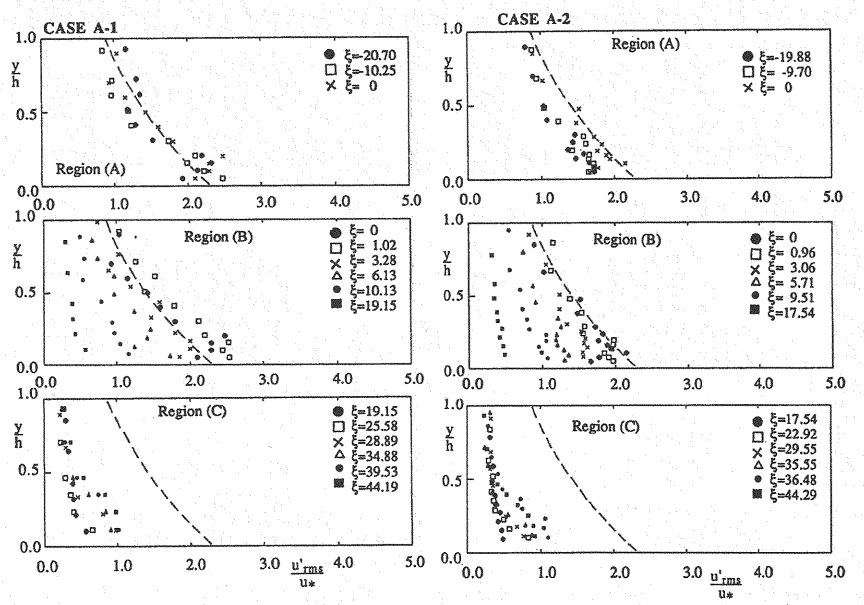

Fig.12(a) Longitudinal change of turbulence intensity by spatial acceleration

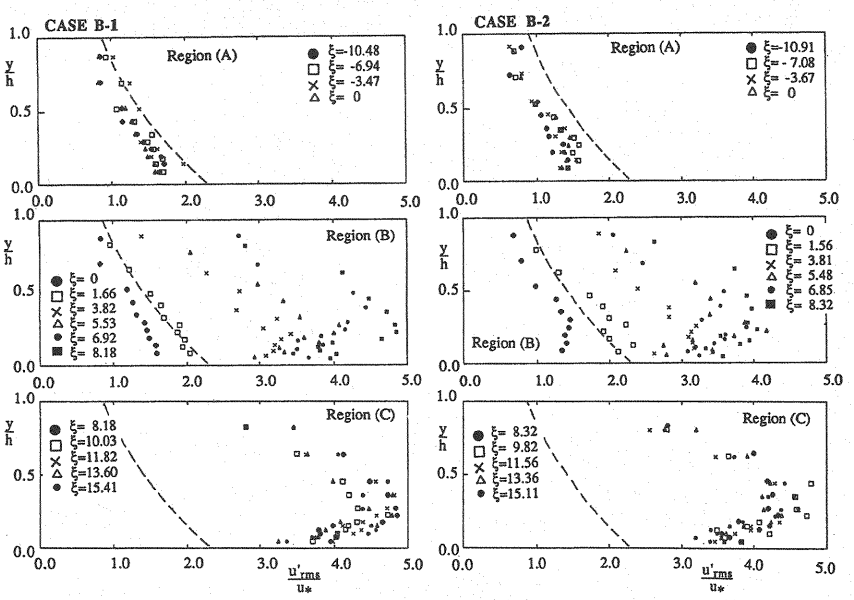

Fig.12(b) Longitudinal change of turbulence intensity by spatial deceleration

Figure 12 shows some examples of the change of the distribution of the turbulence intensity. In the region (A) the vertical distribution of the turbulence intensity normalized by the local shear velocity (u'_{rms}/u_*) is almost equivalent to that for uniform flow (depicted by a dashed curve in Fig.12). In the region (B), the profile of the turbulence intensity becomes shifted from the dashed curve increasingly with the distance x. In the case of acceleration, the normalized turbulence intensity is suppressed. On the other hand, in the case of deceleration, it is promoted. The normalized turbulence intensity near the bed is kept almost constant, but it is evidently promoted particularly in the region far from the bed to make the profile somehow convex. The relative height at which the normalized turbulence intensity has

a maximum rises up with the distance along x. In the case of acceleration, it is difficult to judge whether the bottom value of the normalized turbulence intensity is kept constant or not, but the profile becomes certainly further concave. In the region (B), the spatial derivative of the bed shear stress is rather constant, and thus the spatial change of the profile of the turbulence intensity suggests the relaxation of the turbulence characteristics. The reverse process in the region (C) is ultimately slow.

EXPERIMENT OF SPATIALLY ACCELERATED FLOW AT LHYDREP-EPFL

At LHYDREP-EPFL (Hydraulics Laboratory, Ecole Polytechnique Fédérale de Lausanne, Switzerland), flow measurements were conducted in a large flume by Cardoso et al. (3,4). Since the flume was 41m long and 2m wide, large flow depths could be used. Thus the data of the velocity at the small relative height could be obtained without difficulty. Near the downstream end of the flume, a triangular-shape solitary dune model was set (see Fig.13) to provide the flow with spatial acceleration. The flume was almost horizontal, and the dune model was 2.61m long with an uprising slope of 4.99° In the upstream region of the dune model, the flow was quasi-uniform with the depth of about 35cm.

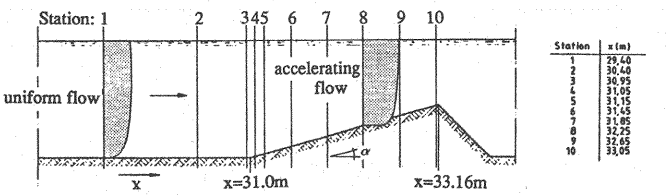

Fig.13 Schenmatic figure of the experiment at LHYDREP-EPFL

Velocity profiles were measured with a Pitot tube at several sections (see Fig.13). The turbulence intensity in the longitudinal direction was measured with a hot film anemometer. Furthermore, the bed shear stress was directly measured by means of a flash-mounted hot film manufactured according to Gust (6) . The output from the instrument was accurately calibrated by using head losses of a testing closed conduit.

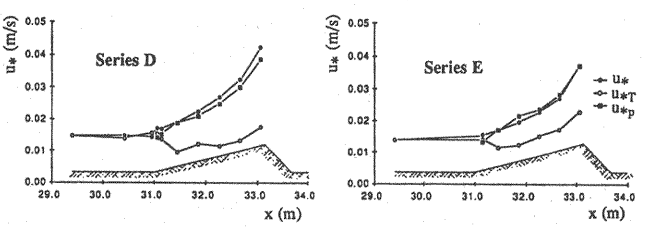

Fig.14 Spatial change of shear velocity along x

The spatial change of the directly measured shear velocity (u_*) is shown in Fig.14. In the figure, the indirect evaluations of the shear velocity are also plotted. One (u_{*T}) is estimated by fitting the log law using the velocity profile from the bed to the surface; while the other (u_{*p}) is estimated by fitting the log law using only the velocity data near the bed. The latter is well consistent with the directly measured shear velocity. That means that the method adopted in the preceding chapter to evaluate the shear velocity has been reasonable.

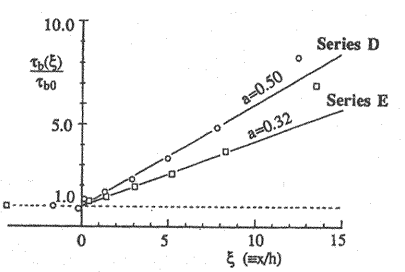

Fig.15 Normalized spatial change of bed shear stress

In Fig.15, the spatial change of the bed shear stress is shown. According to this figure, it can be approximated as

$$\frac{\tau_b(\xi)}{\tau_{b0}} = 1+a\xi \qquad (\xi > 0) \qquad (24)$$

in which $\xi > 0$; τ_{b0}=bed shear stress in the uniform flow region (x<0); $\xi \equiv x/h(x)$; and x=distance along the bed from the upstream end of the dune model.

Figure 16 shows the change of the velocity distribution. The velocity profile becomes more uniform than the log law increasingly from the near-surface region. With the increase of x, the uniform part grows. That is the same tendency to the acceleration case in Fig.11. The data of LHYDREP have more data of the velocity near the bed, and thus we can confirm that the log low is still valid in the wall region, the thickness of which decreases with x.

Figure 17 shows the change of the distribution of the dimensionless turbulence intensity (turbulence intensity divided by the local shear velocity), and this is similar to the data obtained in the small flume of Kanazawa University (see Fig.12).

The data of LHYDREP are significant here in the following two aspects: (1) The bed shear stress was directly measured, and the reliability of the method to evaluate it indirectly using the velocity data near the bed was confirmed; (2) The LHYDREP data were obtained in the much larger flume than the flume at Kanazawa University (5 times in width), and few difference of the results between them confirmed the reliability of the measurements in the small flume.

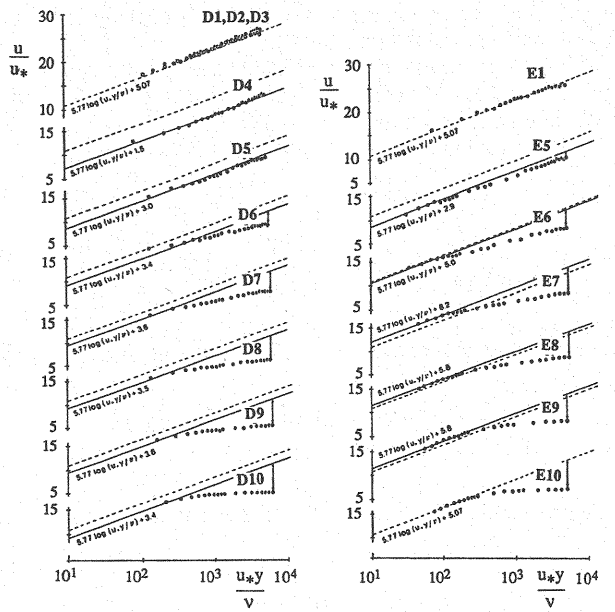

Fig.16 Change of velocity profile by flow acceleration

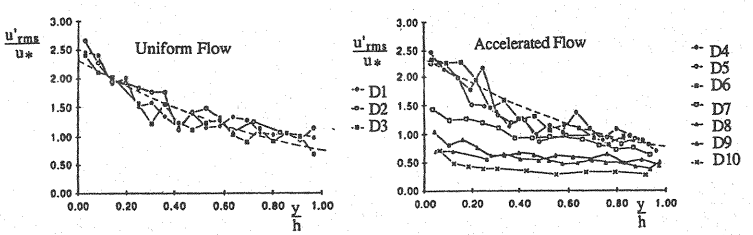

Fig.17 Change of turbulence intensity profile by flow acceleration

APPLICATION OF RELAXATION MODEL TO FLOW WITH SPATIAL ACCELERATION

The flows over ascending and/or descending reaches are accompanied by the spatial acceleration and/or deceleration, respectively, or the bed shear stress increases and/or decreases longitudinally, respectively. The flows treated in the previously mentioned experiments are expected to have too weak spatial acceleration to bring about the direct effect. Thus the degeneration of the flow structure is expected to be brought about by the relaxation effect. In this chapter, the relaxation model for Reynolds-stress distribution, is applied to them.

The spatial change of the bed shear stress is to be expressed as follows:

$$\frac{\tau_b(\xi)}{\tau_{b0}} = \begin{cases} 1 & (\xi < 0) \\ 1+a\xi^p & (0<\xi<\xi_c) \\ s & (\xi>\xi_c) \end{cases} \qquad (25)$$

in which a, p=constants; $s \equiv 1+a\xi_c^p$; and a>0 means the flow acceleration, while a<0 the flow deceleration. The three regions in Eq.25 correspond to the regions (A), (B) and (C) of the flume of the experiments mentioned (see Fig.9).

When the spatial change of the bed shear stress is expressed as Eq.25, the index to represent non-equilibrium, $\Omega(\eta|\xi)$, can be calculated based on Eq.7. The region (A) is regarded as a uniform flow reach, and $\Omega(\eta|\xi)$ in this region is 1.0.

In the region (B), $\Omega(\eta|\xi)$ is calculated as follows:

$$\Omega(\eta|\xi) \equiv \frac{\int_0^{\xi}(\xi-\delta)^p \cdot g_R(\delta|\eta)d\delta + \int_{\xi}^{\infty} g_R(\delta|\eta)d\delta}{1+a\xi^p} \tag{26}$$

The experimental results of LHYDREP suggests p=1. Then Eq.26 becomes simpler:

$$\Omega(\eta|\xi) \equiv \frac{1+a\left\{\xi-\Lambda(\eta)\cdot\left[1-\exp\left(-\frac{\xi}{\Lambda(\eta)}\right)\right]\right\}}{1+a\xi} \tag{27}$$

Furthermore in the region (C), Eq.26 is calculated as follows (for p=1):

$$\Omega(\eta|\xi) \equiv \frac{1+a[\alpha(\eta|\xi)+\beta(\eta|\xi)]}{1+a\xi} \tag{28}$$

in which

$$\alpha(\eta|\xi) \equiv \xi_c\left[1-\exp\left(-\frac{\xi-\xi_c}{\Lambda(\eta)}\right)\right] \tag{29}$$

$$\beta(\eta|\xi) \equiv \Lambda(\eta)\cdot\left[1-\exp\left(-\frac{\xi}{\Lambda(\eta)}\right)\right] + \left[\xi_c-\Lambda(\eta)\right]\exp\left(-\frac{\xi-\xi_c}{\Lambda(\eta)}\right) \tag{30}$$

The calculation was conducted for the condition of the experiments of spatially accelerating flow of LYHDREP. The calculated distribution of Reynolds stress, turbulence intensity and velocity are shown in Figs.18, 19 and 20, respectively.

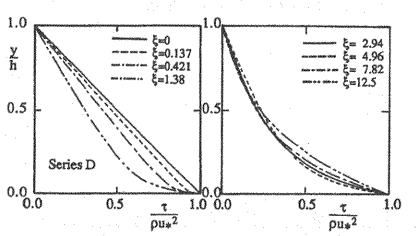

Fig.18 Calculated Reynolds-stress distribution

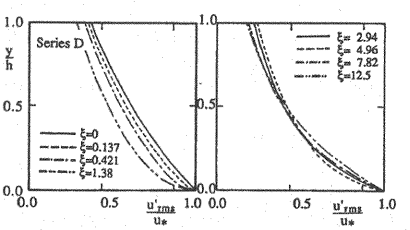

Fig.19 Calculated turbulence intensity

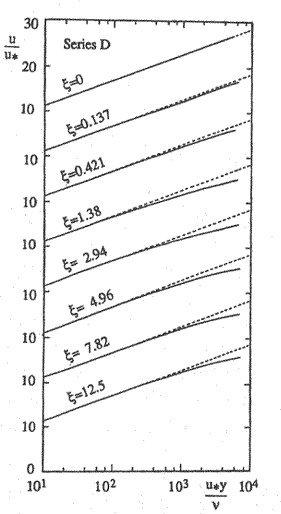

Fig.20 Calculated change of velocity profile

With the increase of ξ, the distributions of the Reynolds stress and the turbulence intensity becomes increasingly concave and the velocity profile normalized by the local shear velocity becomes more uniform than the log law increasingly from the surface region. These tendencies are qualitatively well consistent with the experimental results shown in Figs.16 and 17. For the further large value of ξ, such non-equilibrium tendencies decay and the profile tends to return back to equilibrium one again. That is more evidently recognized when one inspects Eq.28 analytically. When $\xi >> \Lambda(\eta)$, $[1-\exp(-\xi/\Lambda)]$ approaches zero and thus $\Omega(\eta\,|\xi)$ tends to 1.0 as shown below:

$$\Omega(\eta\,|\infty) \rightarrow \frac{1+a[\xi-\Lambda(\eta)]}{1+a\xi} \rightarrow 1 \qquad (31)$$

That suggests the existence of the equilibrium flow with spatial acceleration. In other words, the flow with equi-acceleration can grow equilibrium where the turbulent structure is equivalent to that of uniform flow. In the experimental results, such a re-equilibrium could hardly be recognized, and the non-equilibrium properties grew monotonously with ξ. Fig.21 depicts the variation of the difference between the surface velocity extrapolated by the log law and that of the present model (u_{s0}-u_s), and it emphasizes that the maximum shift (the minimum in Fig.21) of the velocity profile from the log law appears at a finite distance from the upstream end of the acceleration, but it never appears in the case of deceleration.

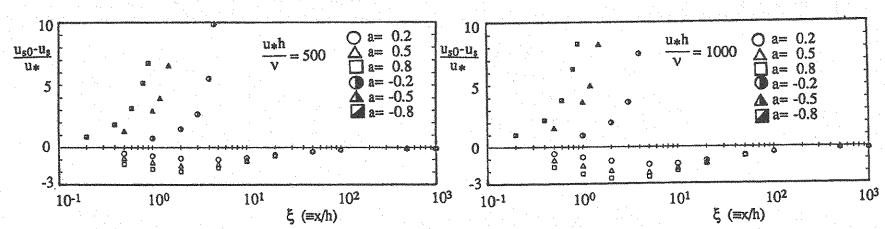

Fig.21 Longitudinal variation of the shift of the surface velocity from the log law

The similar calculations were conducted also for the conditions of the experiments of spatially accelerating and decelerating flows of Kanazawa University. Fig.22a shows the change of the Reynolds-stress distribution in the accelerated reach (region (B)) and in the region with no acceleration but just downstream of the flow acceleration (region (C)). At the downstream end of the region (B), the flow already turns to re-equilibrium but not sufficiently. In the region (C), the Reynolds stress returns back to the equilibrium profile faster in the region with the smaller y/h. Fig.22b shows the change of the Reynolds-stress distribution in the decelerated flow region (region (B)) and in the region without deceleration but just downstream of the flow deceleration (region (C)). In the case of flow with spatial deceleration, the Reynolds-stress distribution becomes more convex with the increase of ξ, and no re-equilibrium process takes place. In the downstream reach where the flow deceleration disappears, the convex non-equilibrium profile returns to the equilibrium one increasingly from the near-bed region.

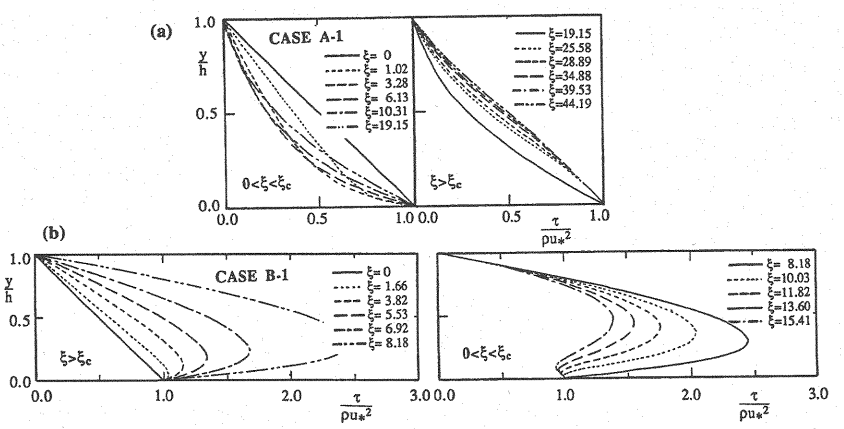

Fig.22 Calculated Reynolds-stress distribution from accelerating and decelerating flows

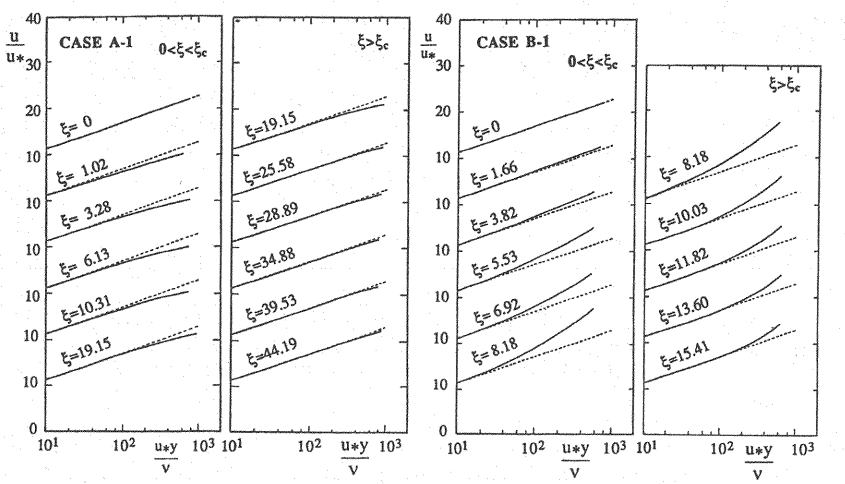

Fig.23 Calculated velocity profiles for accelerating and decelerating flows

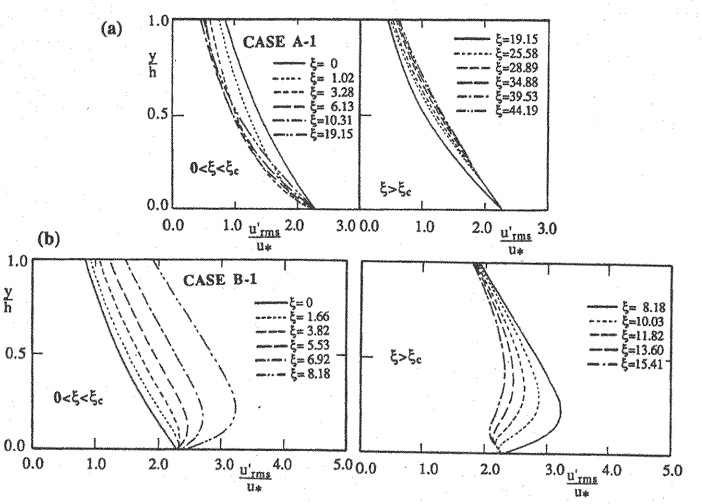

Fig.24 Calculated turbulence-intensity profiles for accelerating and decelerating flows

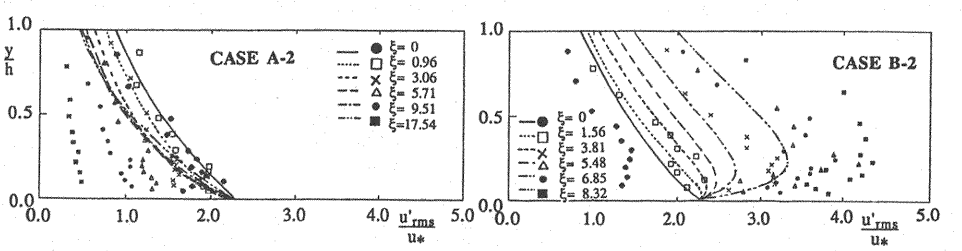

Fig.26 Comparison between the relaxation model and the experimental data - turbulence intensity

Based on the calculated Reynolds-stress distributions, the changes of the velocity profile and the distribution of the turbulence intensities in the regions (B) and (C) were evaluated as shown in Figs.23 and 24, respectively. These calculated results explain the characteristics of the experimental results qualitatively well. The quantitative comparisons between the calculated and the measured profiles are shown in Figs.25 and 26. The effects of the spatial change of flow seem to be underestimated in the

present calculations. That may depend on inaccurate estimations of the relaxation distance. Moreover, it should be investigated whether the impulse response is universal or not.

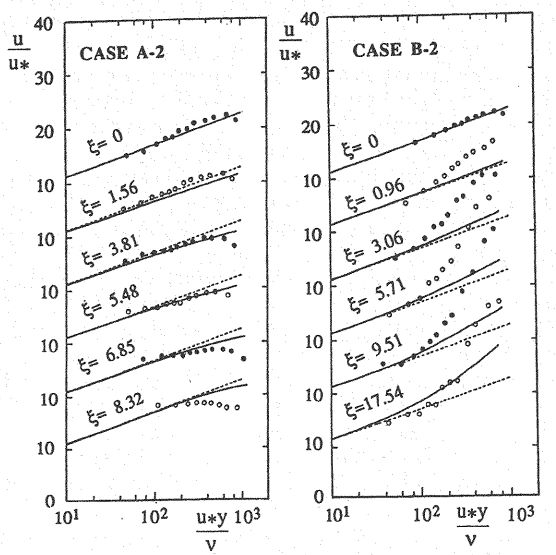

Fig.25 Comparison between the relaxation model and the experimental data - velocity profile

CONCLUSIONS

In this paper, the relaxation model to describe the transition process of the Reynolds stress distribution has been discussed in the first part. The results of this part is summarized as follows:

(1) By focussing the properties that the Reynolds stress adapts the change of the bed shear stress faster in the region near the bed and slower in the region far from the bed, the relaxation model of the Reynolds-stress distribution has been proposed, where the relaxation scale is a function of the relative distance from the bed.

(2) The relaxation model with an exponential type impulse response can describe well the data obtained in the wind tunnel, and the parameter (relaxation distance) has been determined as a function of the relative height.

(3) By applying the mixing length theory to the Reynolds-stress distribution, the velocity profile has been derived and the degeneration from the log law can be explained.

(4) By assuming that the vertical changes of the correlation coefficient of turbulence in the longitudinal and the vertical directions and the ratio of the turbulence intensity in the longitudinal direction to that in the vertical direction are similar even under non-equilibrium and equivalent to those under equilibrium, the turbulence intensity profile is derived from non-equilibrium Reynolds-stress distribution.

(5) The model has been applied to open channel flow with an abrupt change of bed roughness. Practically, the bed shear stress can be assumed to respond to the change of the bed roughness immediately. Thus, the present model makes it possible to calculate the Reynolds-stress distribution, the velocity distribution and the turbulence intensity profiles in the transition process. The calculated results are compared with the recent refined turbulence measurements in open channel flow with an abrupt change of bed roughness. As the result, the impulse response determined based on the classic wind tunnel data could be applied successfully to open channel data without modification.

Measurements of spatially accelerating or/and decelerating flow conducted in the flume have been discussed. The accelerating and the decelerating flows were obtained by ascending and descending slopes, where almost constant spatial derivatives of the bed shear stress were obtained for individual runs. The following characteristics were induced from the experiments:

(1) In an accelerated region, the velocity profile becomes more uniform than the log law in the region far from the bed, and the shift from the log law increases with the longitudinal distance in the region with almost constant spatial derivative of bed shear stress. In the wall region the log law with the universal constants is still valid. In the region with no acceleration but just downstream of the

accelerated region, the velocity profile is still degenerated but gradually returns to the log low. In the case of decelerated flow, the velocity gradient of the region far from the bed becomes greater than that of the log law with the longitudinal distance, though the log-law with the universal constants is still valid in the wall layer, the thickness of which decreases against the longitudinal distance.

(2) The vertical distribution of the turbulence intensity non-dimensionalized by the local shear velocity is degenerated to become more concave by suppression of the turbulence in the core region of flow with acceleration; while it is degenerated to become more convex by promotion of the turbulence in the core region of flow with deceleration. Particularly for deceleration, the bottom turbulence intensity non-dimensionalized by the local shear velocity tends to be constant. The turbulence intensity profile has a tendency to return back to the equilibrium one after the acceleration disappears.

(3) The aforementioned properties could be qualitatively well explained by the relaxation model of the Reynolds-stress distribution, but the model quantitatively underestimates the effects of the change of the bed shear stress. The relaxation model suggests that the velocity profile of flow with constant spatial acceleration tends to equilibrium after a sufficient longitudinal distance. That means that the maximum shift of the profile from the equilibrium one appears at a finite longitudinal distance. Such a tendency never appear for flow with spatial deceleration. In the present experiments, the re-equilibrium profile of flow with spatial acceleration could not be recognized.

As for the flow with spatial acceleration, the large scale flume experiments were conducted at LHYDREP-EPFL. The obtained results are well consistent with the present experiments. The series of the experiments of LHYDREP are significant from the following two aspects in this study: (1) The bed shear stress was directly measured; and the results suggested that the shear velocity is reasonably estimated by applying the log-law with the universal constants only to the velocity data in the near-bed region. (2) The LHYDREP data were obtained in the flume with 5 times width of the flume used in the present experiments, and the same characteristics of flow with spatial acceleration were induced.

The further study should be conducted in order to obtain quantitatively more accurate description of flow with spatial acceleration. One possibility is to improve the evaluation of the impulse response function; and another is more detail direct investigation of turbulent characteristics with more refined flow measurements and devised data analyses (22).

This paper is essentially based on the authors' paper written in Japanese (19), but considerably revised and further results are added herein.

AKNOWLEDGEMENTS

This study started when the first and the second authors stayed at LHYDREP-EPFL (Hydraulic Laboratory, Ecole Polytechnique Fédérale de Lausanne), and Prof. Walter H. Graf, Director, LYDREP-EPFL, kindly advised them to accomplish it. The experiment at LHYDREP was carried out as a part of the second author's doctoral work (3) supervised by Prof. Graf. The third author was engaged mainly in the experiments of Kanazawa University, but he also visited LHYDREP at the final stage of this study to discuss results. All the authors express their sincere gratitude to Prof. Graf for his kind arrangements in this research cooperation.

REFERENCES

1. Antonia, R.A. and R.E. Luxton : The response of a turbulent boundary to a step change in a surface roughness, Part I, *Jour. Fluid Mech.*, Vol.48, pp.721-761, 1971.
2. Antonia, R.A. and R.E. Luxton : The response of a turbulent boundary to a step change in a surface roughness, Part II, *Jour. Fluid Mech.*, Vol.48, pp.737-757, 1972.
3. Cardoso, A. H. : *Doctoral Dissertation*, Ecole Polytechnique Federale de Lausanne, Switzerland, 1990.
4. Cardoso, A.H., W.H. Graf and G. Gust : Spatially accelerating flow in smooth open channel, *Proc. 23rd Congr. of IAHR, Turbulence in Hydraulics*, Ottawa, Canada, Vol.A, pp.7-14, 1989.
5. Coles, D. : The law of the wake in the turbulent boundary layer, *Jour. Fluid Mech.*, Vol.2, pp.191-226, 1956.
6. Gust , G. : Skin friction probes for field applications, *Jour. Geophys. Res.*, Vol.93, 1988.
7. Ishikawa, T. : A fundamental study on sediment transportation in alluvial channels, *Technical Report*, Dept. of Civil Engrg., Tokyo Inst. of Technology, No.24, pp.1-118, 1978 (in Japanese).
8. Jacobs, W. : Umformung eines turbulenzen Geschwindigkeits-Profils, *ZAMM* 19, pp.87-100, 1939 (quoted from "*Boundary-Layer Theory*" by H. Schlichting, 6th ed., McGraw-Hill, pp.615-616, 1968).

9. Kanda, K., Y. Muramoto and Y. Fujita : Turbulent structure of open channel flows with sudden change in bottom roughness, *Proc. 33rd Jap. Conf. on Hydraul.*, JSCE, pp.499-504, 1989 (in Japanese).
10. McLean, S.R. and J.D. Smith : A model for flow over two-dimensional bed flows, *Jour. Hydraul. Engrg.*, ASCE, Vol.112, No.4, pp.301-317, 1986.
11. Murashige, H., S. Matsunashi and H. Kikkawa : Estimation of bed shear stress in the flow with abrupt change of bed roughness, *Proc. JSCE*, No.369/II-5, pp.33-41, 1986 (in Japanese).
12. Nakagawa, H., T. Tsujimoto and S. Murakami : Equilibrium dune profile determined by non-equilibrium bed load transport process, *Proc. 6th Cong. of APD-IAHR*, Kyoto, Japan, Vol.2, pp.99-106, 1988.
13. Nakagawa, H., T. Tsujimoto and Y. Shimizu : Velocity profile of flow over rough permeable bed, *Proc. 6th Cong. of APD-IAHR* , Kyoto, Japan, Vol.2, pp.449-456, 1988.
14. Nezu, I. : Turbulent structure in open-channel flows, *Doctoral Thesis*, Kyoto Univ., 118p., 1977 (in Japanese).
15. Nezu, I., H. Nakagawa, K. Seya and Y. Suzuki : Response of velocity profile and bed shear stress to abruptly changed roughness in open-channel flows, *Proc. Hydraul. Eng.*, JSCE, Vol.34, pp.505-510, 1990 (in Japanese).
16. Nezu, I. and W. Rodi : Open-channel flow measurements with laser Doppler anemometer, *Jour. Hydraul. Eng.*, ASCE, Vol.112, No.5, pp.335-355, 1986.
17. Townsend, A.A. : Equilibrium layers and wall turbulence, *Jour. Fluid Mech.*, Vol.11, pp.97-120, 1961.
18. Townsend, A.A. : The response of a turbulent boundary layer to abrupt change in surface condition, *Jour. Fluid Mech.*, Vol.22, pp.799-822, 1961.
19. Tsujimoto, T., A. H. Cardoso and A. Saito : Open channel flow with variable bed shear stress, *Proc. Hydraul. Eng.*, JSCE, Vol.34, pp.433-438, 1990 (in Japanese).
20. Tsujimoto, T., K. Motohashi and S. Inoue : Transient process of Reynolds-stress distribution due to abrupt change of bed roughness in open channels, *Mem.*, Fac. of Tech., Kanazawa Univ., Vol.22, No.2, pp.15-24, 1989.
21. Tsujimoto, T. and H. Nakagawa : Local rate of bed load transport over a triangular shape dune, *Proc. 4th Congr. of APD-IAHR*, Chiang Mai, Thailand, Vol.1, pp.125-138, 1984.
22. Tsujimoto, T. and A. Saito : Open channel flow with spatial acceleration or deceleration, *KHL-Progressive Report*, No.1, Kanazawa Univ., No.1, pp.13-30, 1990.

APPENDIX - NOTATION

The following symbols are used in this paper:

a	= constant;
A, B	= constants;
f	= frequency;
Fr	= Froude number;
g	= gravity acceleration;
$g_R(\delta \mid \eta)$	= impulse response of Reynolds stress at the relative height η;
h	= flow depth;
H	= difference of the elevations of the uniform regions upstream and downstream of the ascending (or descending part);
i_b	= bed slope;
K_{uv}	= u'_{rms}/v'_{rms};
ℓ, ℓ^*	= mixing length and its normalized value by depth;
L	= length of the ascending (or descending) part in the flume;
p	= constant;
r_T	= correlation of turbulence between the longitudinal and vertical components;
$r_{T*}(\eta)$	$\equiv r_T(\eta)/(1-\eta)$;

Re	= Reynolds number;
s	= constant;
u	= local velocity;
u_*	= shear velocity;
u_{*T}, u_{*p}	= shear velocity estimated by fitting the log law using the velocity profile from bed to the surface; and that by fitting using the velocity data only near the bed;
u'_{rms}, v'_{rms}	= turbulence intensities in longitudinal and vertical directions;
U	= depth-averaged velocity;
x	= longitudinal distance;
y	= vertical distance from the bed;
$\alpha(\eta \mid \xi)$, $\beta(\eta \mid \xi)$	= defined by Eqs.29 and 30, respectively;
β	$\equiv u_{*2}/u_{*1}$;
ν	= kinematic viscosity;
κ	= Kármán constant;
Π	= Coles' wake-strength parameter;
$\Lambda(\eta)$	= relaxation distance of turbulent flux at η normalized by flow depth;
ϕ_1, ϕ_2	= velocity profiles to correspond to the inner and the outer regions, respectively;
$\Theta(\eta \mid \xi)$	= $\Omega(\eta \mid \xi)$ for the case of abrupt change of bed roughness;
$\Omega(\eta \mid \xi)$	= defined by Eq.7 which represents change of the Reynolds-stress profile from the equilibrium triangular shape;
$\tau(\eta \mid \xi)$	= Reynolds-stress distribution at ξ;
ξ	$\equiv x/h$;
η	$\equiv y/h$;
$\tau_b(\xi)$	= longitudinal change of bed shear stress; *and*
$\psi_b(\xi-\delta)$	$\equiv \tau_b(\xi-\delta)/\tau_b(\xi)$

(Received July 26, 1990; revised November 1, 1990)